

Characterization of broadband dispersion behaviors of wedge waves with different boundary conditions by laser ultrasound technique

Wen-Chih Wang[†], Che-Hua Yang¹

(Institute of Mechanical and Electrical Engineering, National Taipei University of Technology)

Abstract

This paper is focused on the experimental observation of the broadband dispersion behaviors of antisymmetric (ASF) flexural modes with different boundary conditions. Dispersion behavior of ASF modes propagating along wedge tips with different boundary conditions, namely in the vacuum and with fluid loadings, are studied. It is the purpose of the paper to study the behaviors of ASF modes propagating along wedges with different boundary conditions with experimental study based on a broadband laser ultrasound technique. It is found out that the effect of fluid loading is to reduce the ASF phase velocity, and the reduction ratio is found to be a constant value for the investigated frequency range. It is also found out that an immersed ASF mode can propagate only with a phase velocity smaller than wave velocity of the fluid.

1. Introduction

Wedge waves with their displacement field anti-symmetric about the mid-apex-plane are called anti-symmetric flexural (ASF) modes. Fig.1. shows a typical motion type for an ASF mode. Research in the properties of ASF modes propagating in wedge wave guides was initiated by Lagasse[1] in early 1970's. Based on their research, the relation between the speeds of ASF modes and the Rayleigh wave speed is frequently used for the isotropic materials. Lagasse's empirical formula predicts the phase velocity of ASF mode, V , to be proportional to the surface wave speed [2] as: $V = V_R \sin(n\theta)$, where V_R is the surface wave speed, θ is the apex angle and $n=1$ for the fundamental ASF mode. From then on, wedge waves propagating along isotropic wedges have been studied on the effects of material properties, apex truncations [2][3], apex angles [4][5], and fluid loading effects [5][6]. This research aims at the effects of the fluid loading for the ASF by using broadband LUT.

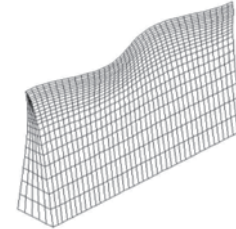


Fig. 1 Motion pattern for an ASF mode

2. Theory

Reminding the approximate theory of elastic waves in immersed solid wedges, which is developed by Krylov[6] using geometrical acoustics approach methods. The velocities of WWs propagating along the tip without fluid loading are determined as follow:

$$C_{Vn} = C_p n\theta / \sqrt{3} \quad (1)$$

where V means in the air, n is the mode number of wedge waves, $C_p = 2C_t(1 - C_t^2/C_l^2)^{1/2}$ is so called plate wave velocity, C_t and C_l are shear and longitudinal acoustic waves velocities, θ is the wedge apex angle.

For the cases with fluid loading, the waves' velocities(C) are as follow:

$$\int_0^{B\eta^2} \left[\frac{B}{z} \operatorname{Re} \left(1 + \frac{\rho_f}{\rho_s} \frac{1}{z\sqrt{(B/z) - (C_t^2/C_f^2)}} \right) - \frac{1}{\eta^2} \right] dz = \pi n\theta \quad (2)$$

where $B = \sqrt{3}C_t / \sqrt{C_l^2 - C_t^2}$, $z = k_l d = x\theta\omega / C_l$ and $\eta = C / C_l$. The relation between the mass densities of liquid and solid have been taken into considered.

Although the approximate solutions from geometrical acoustics approach methods can only used for apex angle smaller than 13 degree, but the errors for large apex angles are expected to be the same for immersed wedges and for wedges in vacuum. Therefore, they will cancel each other when we consider the ratio C_L / C_V .

3. Experiments

A broadband laser ultrasonic technique (LUT) is used for the broadband dispersion measurement of the ASF modes travelling along wedge tips with

[†] Email: chyang@ntut.edu.tw

different boundary conditions. The experimental configuration consists of a Nd-YAG pulsed laser for ultrasonic wave generation and a laser-based acoustic wave detection system with photoreceiver. The dispersion curves' bandwidth in this paper is up to 12MHz.

4. Results and discussions

Fig.2 to Fig 4 are WWs dispersion curves with or without fluid loading in different apex angles and materials.

In Fig.2, there are six ASF modes and one surface wave mode can be observed and it has well agreement with Lagasse's empirical formula. Compare the WWs with different boundary condition, it is found that the fluid loading reduces the phase velocity of ASF modes with a constant ratio for all frequencies (A_1 mode with 19.2%, A_2 mode with 8.3% and A_3 mode with 4.3%). And the immersed WWs can only propagate with phase velocity smaller than wave velocity of the fluid.

All the phenomenon mentioned above can also be observed in wedges with different apex angles ($16^\circ, 25^\circ, 30^\circ, 40^\circ$) or different materials (Brass, Al).

Fig.5 shows the agreements between broadband experimental results and approximate solutions in ref 1. The fluid loading effect is a function of apex angle. From Fig.5, we can also find the fluid loading difference in different materials, the difference comes from the density variation ($D_{Brass}=8.4 \text{ g/cm}^3, D_{Al}=2.7 \text{ g/cm}^3$).

5. Conclusions

Broadband dispersion behaviors of ASF modes with different boundary conditions are characterized by LUT. It is found out that fluid loading effect reduces the ASF phase velocity, and the reduction ratio is found to be a constant value for the investigated frequency range. An immersed ASF mode can propagate only with have a phase velocity smaller than wave velocity of the fluid. Fluid loading ratios are affected by apex angle and the density difference between wedge and the immersion fluid.

References

1. P. E. Lagasse, I. M. Mason and E. A. Ash: IEEE Trans. Sonics and Ultrasonics, Vol. **SU-20**(2), 143 (1973).
2. J. McKenna. And G. D. Boyd: IEEE Transactions on Sonics and Ultrasonics, Vol. **Su-21**, No, 3 178-186 (1974).
3. M. de Billy and A. C. Hladky-Hennion: Ultrasonics. **37**, 413-416 (1999)
4. J. Jia and D. Auribault : IEEE Ultrasonics

Symposium 637-640 (1993).

5. M. de Billy : J. Acoust. Soc. Am. **100**(1), 659-662 (1996).
6. V. V. Krylov : J. Acoust. Soc. Am. **103**(2), 767-770 (1998).

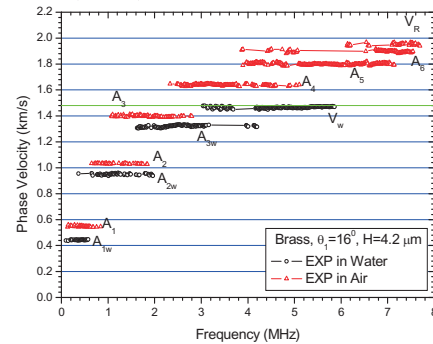


Fig. 2 Measured dispersion curves for the Brass wedge with $\theta=16$ in different boundary conditions.

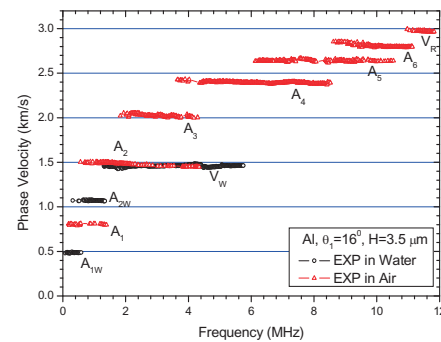


Fig. 3 Measured dispersion curves for the Al wedge with $\theta=16$ in different boundary conditions.

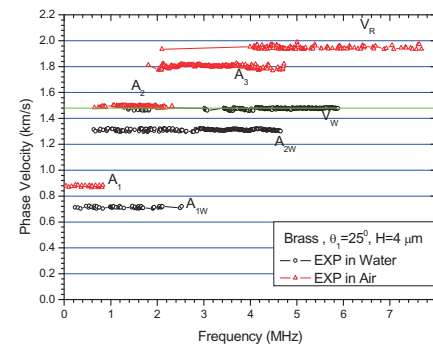


Fig. 4 Measured dispersion curves for the Brass wedge with $\theta=25$ in different boundary conditions.

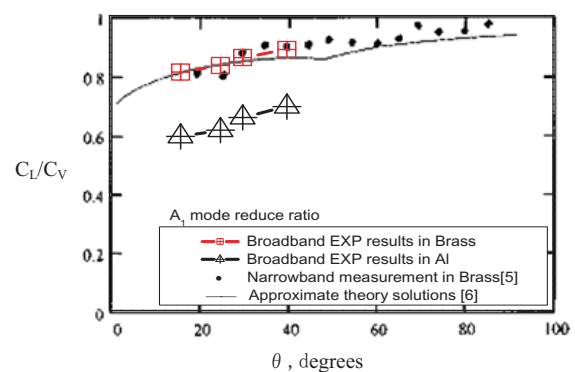


Fig. 5 Experimental variations of the ratio C_L/C_A with respect to the apex angle.